JOURNAL OF APPLIED ELECTROCHEMISTRY 22 (1992) 687–692

Scale-up effects in modelling a full-size zinc electrowinning cell

G. W. BARTON, A. C. SCOTT

Department of Chemical Engineering, The University of Sydney, NSW 2006, Australia

Received 24 July 1991; revised 16 November 1991

The scale-up of a mathematical model of a (10 dm^3) pilot-plant zinc electrowinning cell is considered. All scale-up effects considered were relatively small in magnitude and their inclusion required only readily available full-size cell data. Excellent agreement was obtained between the model predictions and experimental results from an (instrumented) operational full-size cell.

1. Introduction

As 80% of the power requirements for an electrolytic zinc refinery are associated with the electrowinning process, it is economically important to run the cellroom as close to optimum operating conditions as possible. Such operating conditions can be determined for a specified objective function (in this case, minimizing the energy required per tonne of zinc produced) and set of plant operational constraints, given the availability of a validated mathematical model of the electrowinning cells used. As a first step to achieving this objective for the cellroom at the Electrolytic Zinc Company (EZ), Hobart, Australia, a series of experiments were conducted to investigate the major factors affecting the efficiency of zinc electrowinning [1]. These experiments were conducted in 10 dm^3 cells using a high purity industrial zinc sulphate solution. A dynamic mathematical model for these pilot-plant cells has been developed [2]. This model consists of a set of 95 equations comprizing mass balances, an overall energy balance, thermodynamic and kinetic equations, electrochemical and mass transfer equations and correlations for electrolyte conductivity and density. A comparison of the steady-state predictions from this model and the experimental results gave an average (absolute) error of 0.6% and 1.4%, respectively, for the cell current efficiency and specific power consumption. This present paper describes how the pilot-plant model was modified to make it applicable to full-size cells. The final paper in this series will show how the full-size cell model can be used to look at the economic optimization of both existing and proposed alternative electrowinning circuits.

Apart from changing the electrode areas and electrolyte volume to full-size cell values, the following possible scale-up modifications to the pilot-plant model were also considered.

(i) Recalibration of the water evaporation equation.
(ii) Modelling of cell cooling coils and external cooling towers.
(iii) Incorporation of the busbar voltage losses.
(iv) Inclusion of manganese scale effects.
(v) Effect of bubbles on both mass transfer and cell voltage.
(vi) Modelling of cell hydrodynamics.

2. Scaling-up of the pilot-plant cell model

Each of the above modifications will be discussed in turn. The same nomenclature is used here as in the previous description of the pilot-plant cell model [2].

2.1. *Scaling-up of the cathode area and cell volume*

This was simply achieved by increasing the cathodic surface area to 1.22 m^2 and the number of cathodes to 44 (to give a total cathodic area of 53.7 m^2). The cell volume was increased to 3900 dm^3.

2.2. *Recalibration of the evaporation equation*

As in the pilot-plant model, it is assumed that only water is lost through evaporation, with the rate of evaporation being described by the equation

$$r_{\text{evap},H_2O} = K_{\text{evap}} A_s (p_s - p_w) \quad (1)$$

where: K_{evap} = evaporation constant (mol $m^{-2} s^{-1}$ (mm Hg)$^{-1}$); A_s = surface area of the air-electrolyte interface = 2.87 m^2; p_s = saturated vapour pressure of water (mm Hg); and p_w = working (or atmospheric) vapour pressure of water (mm Hg).

A series (of seven) full-size cell sulphate ion balances showed an average 2% increase between the feed and overflow volumetric flowrates. An increase in volume can occur if the decrease in electrolyte density between the feed and overflow streams outweighs the loss of water through evaporation and reaction at the anode. All other things being equal, the proportion of water reacting at the anode will not vary between the pilot-plant and full-size cells. The proportion of water lost due to evaporation is, however, considerably less for a full-size cell, primarily because of its lower surface area to volume ratio (0.073 m^{-1} compared to 4.89 m^{-1} for the pilot-plant cell). Using the average operating conditions for these seven experiments, and requiring a 2% increase in volumetric flow across the cell, the

0021-891X/92

full-size cell model was solved using the SPEEDUP package [3] for the evaporation constant. The value obtained ($K_{evap} = 2.5 \times 10^{-5}$) was an order of magnitude lower than that for the pilot-plant cells. This difference was large but not entirely unexpected. Calculations by Hills and Szekely [4] have shown that under conditions where vapour (from a liquid surface) condensation occurs, the effective mass transfer coefficient (i.e. the evaporation constant) can be a strong function of temperature. Experimental data, for example [5], have tended to confirm these predictions, although they have shown that system geometry can also play an important role. Use of a constant value for K_{evap} is warranted here on the basis that the model predictions for both current efficiency and power consumption are quite insensitive to this parameter [2].

2.3. *Modelling of the cooling coils*

In the EZ cellroom, over half the total number of cells are contained in 24 identical cascades of six cells each. Each cell is fed independently with feed solution with the spent electrolyte overflowing into the following cell. The last cell in each cascade discharges to the spent storage tanks. Each cell in a cascade contains a set of cooling coils, and consequently the energy balance equation for such a cell needs to have a term included to account for the heat extracted (q_{coil} in watts) by the cooling coils. This term may be calculated by including the following equations

$$q_{coil} = n_{coil} A_{coil} U \Delta T_{LM} \quad (2)$$

$$q_{coil} = n_{coil} m_{coil} C_p \Delta T_{coil} \quad (3)$$

where: n_{coil} = number of coils per cell (= 5); A_{coil} = area of a coil (= 0.25 m^2); U = overall heat transfer coefficient (W m^{-2} K^{-1}); ΔT_{LM} = log mean temperature difference between the electrolyte and the cooling water (K); m_{coil} = flowrate of water through a coil (kg s^{-1}); C_p = heat capacity of water (= 4200 J kg^{-1} K^{-1}); and ΔT_{coil} = temperature rise of the water on passing through a coil (K).

The value of the heat transfer coefficient was estimated using data collected from the cellroom over a range of cooling water flows and cell and cooling water temperatures [6]. The average value for U of 890 W m^{-2} K^{-1} was used in the model of a cascade cell. Although the estimated heat transfer coefficient was relatively inaccurate (the standard deviation of the thirteen values obtained was 120 W m^{-2} K^{-1}), the sensitivity of the model to changes in U is quite small.

2.4. *Modelling of the cooling towers*

The remaining cells in the EZ cellroom are cooled by recirculating part of the spent electrolyte (the remainder leaving the circuit) through cooling towers. In this arrangement, the fresh feed is added to the recirculated spent. The use of cooling towers, rather than cooling coils, is the most common means of removing heat in modern cellrooms.

In cases where cooling is provided by cooling towers, heat and mass balances are performed not over a single cell but over the entire circuit. Under steady-state conditions, the quantity of heat removed in the cooling towers (Q_{tower} in watts) will equal the excess heat generated in all of the cells

$$Q_{tower} = Q_e + Q_f - Q_l - Q_c - Q_r - Q_d \quad (4)$$

where: Q_e = electrical energy input; Q_f = specific heat content of the feed electrolyte; Q_l = heat of evaporation (of water from the cell surfaces); Q_c = (non-evaporative) heat lost from the cells to the atmosphere; Q_r = heat from reaction(s); and Q_d = specific heat content of the spent electrolyte.

When the recirculating electrolyte passes through the cooling towers, its temperature is reduced both by evaporative cooling and convective losses to the surrounding air. The quantity of water evaporated from the electrolyte (M_{tower} in kg s^{-1}) may be calculated using the expression

$$M_{tower} = \alpha Q_{tower} / \lambda \quad (5)$$

where α is the proportion of the total cooling caused by evaporation (generally of the order 0.5–0.7) and λ is the latent heat of evaporation of water (2260 kJ kg^{-1}).

The results from a steady-state model of a recirculating cellroom that includes cooling tower behaviour is one of the application examples that will be presented in the final paper of this series.

2.5. *Incorporation of busbar voltage losses*

The total cell voltage (V_{cell} volts) is calculated by summing the voltage drops for the electrodes and across the solution between the electrodes ($E_{solution}$)

$$V_{cell} = |E_c| + |E_a| + E_{solution} + E_{loss} \quad (6)$$

where E_c and E_a are the cathode and anode potentials, respectively. E_{loss} is a measured correction term which accounts for the voltage loss across the busbars, contacts and the manganese scale on the anode surface. In the model of the pilot-plant cell, this loss term was set to zero since the cell voltage was measured directly from the cathode to the anode. Voltage measurements in the EZ cellroom, however, include all these effects and E_{loss} can be as high as 0.3 V. The voltage loss across the busbars, electrode contacts and the cathode headbars (E_1) was modelled using

$$E_1 = R_1 I_c \quad (7)$$

where I_c is the total cathodic current (A) and R_1 is a total resistance (Ω). The value of R_1 was measured for the various cell types used at EZ [6]. For a cascade cell, for example, the average value obtained for R_1 was 9.72×10^{-6} Ω.

2.6. *Effect of manganese scale*

The voltage loss across the manganese scale on the anode (E_2) was calculated using an expression analogous to Equation 7, except that the current density rather than the total current must be used. That is,

$$E_2 = R_2 i_a \quad (8)$$

Table 1. Comparison of experimental and model results for a full-size cell

Experiment	*1*	*2*	*3*	*4*	*5*	*6*
Cell conditions						
Zinc ($g\,dm^{-3}$)	52.9	51.5	49.9	79.8	52.0	51.2
Acidity ($g\,dm^{-3}$)	167.5	163.5	171.9	130.0	176.8	174.3
Temperature (°C)	39.0	39.6	40.9	40.2	39.9	34.9
Current density ($A\,m^{-2}$)	335	346	357	346	476	320
Deposition time (h)	71.8	71.9	71.7	47.2	47.2	72.0
Current efficiency (%)						
Experimental (ε_e)	92.6	93.0	93.6	94.4	92.2	93.9
Model (ε_m)	93.3	92.4	92.0	96.5	93.7	93.0
$\Delta = \varepsilon_e - \varepsilon_m$	−0.7	0.6	1.6	−2.1	−1.5	0.9
Power ($kWh\,tonne^{-1}$)						
Experimental (P_e)	2792	2772	2730	2810	2879	2730
Model (P_m)	2706	2748	2761	2681	2853	2706
$\Delta = P_e - P_m$	86	24	−31	129	26	24
Cell voltage (V)						
Experimental (V_e)	3.154	3.145	3.120	3.236	3.237	3.129
Model (V_m)	3.080	3.098	3.099	3.157	3.263	3.070
$\Delta = V_e - V_m$	0.074	0.047	0.021	0.079	−0.026	0.059

where i_a is the anodic current density ($A\,m^{-2}$) and R_2 is a representative 'resistance'. At EZ, cellroom measurements [6] indicated that halfway through the anode cleaning cycle, the voltage drop caused by the manganese scale was approximately 0.15 V at a current density of $400\,A\,m^{-2}$. This is equivalent to an R_2 value of $3.72 \times 10^{-4}\,\Omega\,m^2$.

In the full-size cell model, the value of E_{loss} is calculated by adding together E_1 and E_2.

2.7. *Bubble effects*

Since the electrodes in a full-size cell are ten times as long as those in the pilot-plant cell, then all other things being equal, ten times the (bubble) gas volume will be passing through the electrolyte at the top of the cell. In modelling this change, it must be pointed out that bubble effects are still being actively debated in the literature and general models describing combinations of various effects in industrial cells cannot, at present, be considered reliable. However, it was previously assumed for the pilot-plant cell model [2] with regard to mass transfer at the cathode, that the dominant mechanism is the micro-convective effect of bubbles breaking away from the surface (rather than natural convection or the macro-convective effect of bubbles moving through the bulk electrolyte). If this assumption is made, then the increased length of the electrodes should have little effect and the equations used in the pilot-plant model should be equally applicable in the full-size cell model. The level of agreement between the full-size cell experimental data and model results (see Table 1) would seem to indicate that modelling bubble effects on the basis of this simplifying assumption is adequate (if not completely correct at a mechanistic level).

Bubbles may be regarded as insulating spheres which, when accumulated between the electrodes, contribute to the solution resistance by effectively reducing the cross-sectional area for current flow. A number of equations that relate the gas voidage to the increase in solution resistance have been developed (Sides [7] provides a good summary of these). The best known of these is the Maxwell equation which gives the ratio of electrolyte conductivity with bubbles present (σ_b in $S\,m^{-1}$) to that when no bubbles are present (σ) as a function of the bubble void fraction (f),

$$\sigma_b/\sigma = (1 - f)/(1 + f/2) \qquad (9)$$

The Maxwell equation requires a value for the gas voidage, which depends on the volumetric gas flowrate and, thus, on the superficial gas velocity. Kreysa and Kuhn [8] measured gas voidage as a function of superficial gas velocity for a range of gas-solution systems. Their results for oxygen and hydrogen in 20% sulphuric acid were used in the present calculations.

For oxygen evolution at the anode, the superficial gas velocity (u_0 in $m\,s^{-1}$) may be calculated using

$$u_0 = V_{O_2}/A_x = (RTI)/(pn_{O_2}FA_x) \qquad (10)$$

where: V_{O_2} = volume of oxygen produced ($m^3\,s^{-1}$); A_x = cross-sectional area between the electrodes (m^2); R = gas constant ($8.314\,J\,mol^{-1}\,K^{-1}$); T = electrolyte temperature (K); I = current through the anode (A); p = pressure (Pa); n_{O_2} = number of electrons transferred per molecule (=4); and F = Faraday constant ($96\,500\,C\,mol^{-1}$).

Assuming representative values for EZ full-size cells of A_x ($0.03\,m^2$), T (308 K), I (500 A) and p (1.01×10^5 Pa) gives a superficial oxygen gas velocity of $1.09 \times 10^{-3}\,m\,s^{-1}$, which is equivalent [8] to an (oxygen) gas voidage of approximately 0.03. Therefore, the voidage would be expected to increase from zero at the bottom of a full-size cell electrode to a maximum of 0.03 at the top. If an average voidage of 0.015 is used, Equation 9 indicates that this is equivalent to an average decrease in electrolyte conductivity of about 2% (with a 4% decrease at the top of the cell).

Using the same representative conditions as above,

and assuming that 10% of the cathodic current is used in the production of hydrogen, it can be shown [6] that hydrogen evolution has a negligible effect on the overall gas voidage and, thus, on the electrolyte conductivity.

The value calculated above for the change in electrolyte conductivity due to the presence of bubbles (a 4% decrease at the top of the cell) is lower than the 6% decrease experimentally measured [6] at the top of a similar sized cell. This discrepancy could be due in part to the recirculation occurring between the electrodes which would tend to increase the mean value of the gas voidage. However, an average decrease of 2% in electrolyte conductivity is only equivalent to an increase in cell voltage of approximately 10 mV at a current density of $500\,A\,m^{-2}$. As the inclusion of bubble effects significantly increases the complexity of the model, but provides only a small increase in accuracy, these effects were not included in the EZ full-size cell model. It should be realized that in other situations (for example, significantly larger cathodes), the inclusion of such effects may well be warranted.

2.8. *Modelling of cell hydrodynamics*

The pilot-plant cells were modelled on the assumption that the cell contents were well-mixed. For full-size cells, however, very little information was available on likely cell hydrodynamics. Measurements by Rawling and Costello [9] on a full-size copper electrowinning cell had indicated that a significant amount of bypassing (that is, the rapid movement of electrolyte from the feed to the cell overflow) might be expected. In each cascade (of six cells) at EZ, the feed to each cell is made up of both the overflow from the previous cell together with more fresh feed. Consequently, the flowrate progressively increases down a cascade, and each of the six cells could potentially have quite different hydrodynamics. Much less differences were expected in the recirculating cell arrangements at EZ, where each of the six cells are essentially independent of each other, having a separate feed line and returning spent electrolyte to a common launder.

Preliminary profiles of the electrolyte temperature, acidity and conductivity in both cascade and recirculating cells indicated that while the mixing induced by the generation of bubbles at the electrodes was considerable, the cells were not perfectly mixed. Consequently, lithium (as lithium chloride) tracer tests were conducted on the first, third and last cells of a cascade and on one recirculating cell. Care was taken to ensure that the addition of the tracer caused as little disturbance to a cell as possible. The density of the tracer solution was adjusted (by the addition of zinc sulphate) to be the same as that of fresh feed, and its addition (over a one minute period) was at the same rate as that of fresh feed (which was turned off while the tracer was added). Samples were taken at eight locations in each cell and lithium analyses made using Atomic Absorption Spectroscopy [6].

All the available data indicated that a hydrodynamic model consisting of two well-mixed tanks in parallel might be adequate. The most general version of such a two-tank model is shown in Fig. 1 and involves four parameters:

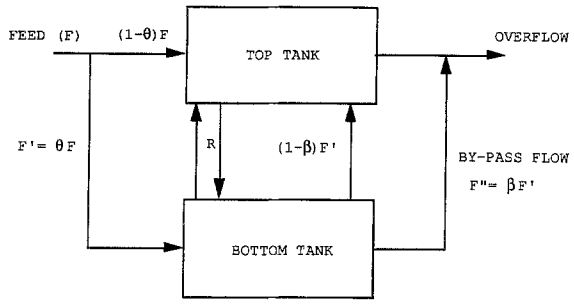

Fig. 1. Proposed two-tank hydrodynamic model of a full-size cell.

(i) The volume of the top tank (V_t). The volume of the bottom tank (V_b) is given by $V - V_t$ where V is the total volume of electrolyte in the cell.
(ii) The fraction (θ) of the fresh feed going to the bottom tank.
(iii) The recirculation rate (R) between the two tanks.
(iv) The fraction (β) of the flow to the bottom tank that by-passes the top tank.

In line with physical considerations, V_t was taken as the volume of electrolyte in the electrode region (that is, above the level of the bottom of the electrodes) with V_b taken as the volume between the bottom of the electrodes and the floor of the cell. This reduced the problem of fitting the experimental tracer data to a search over three parameters. For each tank, an unsteady-state tracer balance described the way that the tank concentration (C_{tank} in $mg\,Li\,dm^{-3}$) varied with time;

$$V_{tank}(dC_{tank}/dt) = \Sigma(F_{in}C_{in}) - \Sigma(F_{out}C_{tank}) \qquad (11)$$

In the above equation, F_{in} and C_{in} are the flowrate and tracer concentration of an inflowing stream, respectively, while F_{out} is the flowrate of an outflowing stream. The SPEEDUP package [3] was used to solve a (non-reactive) dynamic model of the two-tank system and thus find the parameter values that gave the best fit between the model predictions and the experimental data. For each of the four cells considered, an excellent fit was obtained when all the feed went to the bottom tank (that is, $\theta = 1$) and no electrolyte from the bottom tank by-passed the top tank (that is, $\beta = 0$). A single recirculation rate (R) of 40–50 $dm^3\,min^{-1}$ could be used for all three cascade cells considered, while for the recirculating cell, a somewhat higher value ($R = 140\,dm^3\,min^{-1}$) was required. Figure 2 compares the experimental tracer results with the two-tank model simulation results for the overflow from the first cascade cell.

The dynamic equations describing the behaviour of the single tank model, or the upper tank in the two-tank model, are essentially the same as those presented previously for a single well-mixed electrolytic cell. The equations describing the lower tank in the two-tank model are similar but contain no electrolytic reaction

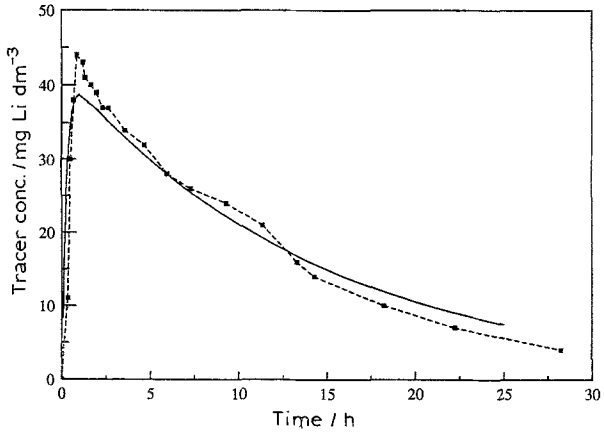

Fig. 2. Comparison of tracer test results with two-tank model. Key: (– – ■ – –) experimental results; (———) two-tank model.

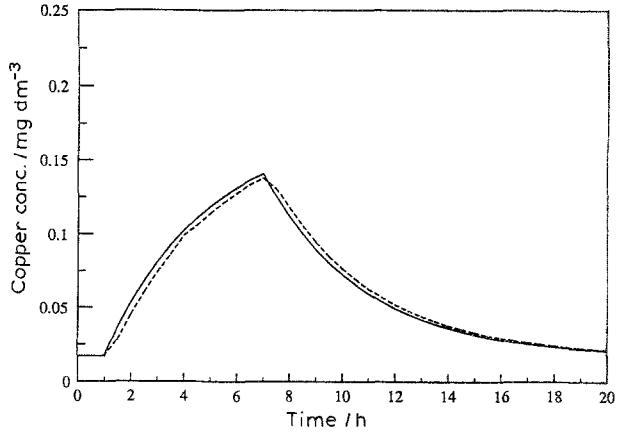

Fig. 4. Comparison of one and two-tank simulations of copper 'slug'. Key: (– – – –) two-tank model; (———) one tank model.

terms. As there is no reaction occurring in the lower tank of the two-tank model, the steady-state results obtained from the one and two-tank models are identical. The two models do, however, produce slightly different dynamic responses as shown in Figs. 3–5, all of which are for the first cascade cell. Figure 3 compares the lithium tracer overflow predictions from the one and two-tank models, while Fig. 4 compares the exit copper concentrations from the two models when each is subjected to a 6 h long square pulse (Cu^{2+} jumping from 0.064 mg dm^{-3} to 0.64 mg dm^{-3} after 1 h and returning to it's original value after 7 h). Both figures show little difference between the (non-reactive) dynamic responses of the two models as far as exit concentration goes. Finally, Fig. 5 shows the way current efficiency varies with time when a cell is subjected to a step change (from 0.10 to 0.07 dm^3 s^{-1}) in feed flowrate. Similar results would be expected for the other cells. If the dynamics for the first cell in a cascade (characterized by a low feed flowrate and long residence time) are well approximated by a single well-mixed reactor, then other cells with higher feed flowrates would also be expected to be modelled by such a system.

3. Validation of the full-size cell model

In the EZ cellroom, there are two full-size 'monitored' cascade cells which can be used for carrying out experiments under normal cellroom operating conditions. These cells have extra instrumentation to assist in both data collection and control of the cell operating conditions [6]. Table 1 compares the results from six steady-state experiments carried out in these cells with the predictions from the full-size cell model. The experimental results quoted are the average values over the course of each run.

There is very good agreement between the experimental and model predicted current efficiencies. However, the cell voltages shown in Table 1 would indicate that the model is consistently predicting a lower value (on average, about 40 mV). The reason for this slight difference is not known. As a result of this discrepancy in cell voltage, the model also slightly underpredicts the power consumption (on average, by about 45 kWh tonne^{-1}). It should be realized in comparing these results, however, that the full-size model used was simply the pilot-plant model scaled-up to include the effects discussed previously in this paper, i.e. there was no fitting of the model to any experimental full-size cell results.

Although there is a small systematic error in the calculation of the cell voltage, this is not large enough to affect the predictive ability of the full-size cell model. Given the difficulty of maintaining feed and cell operating conditions steady for long periods of

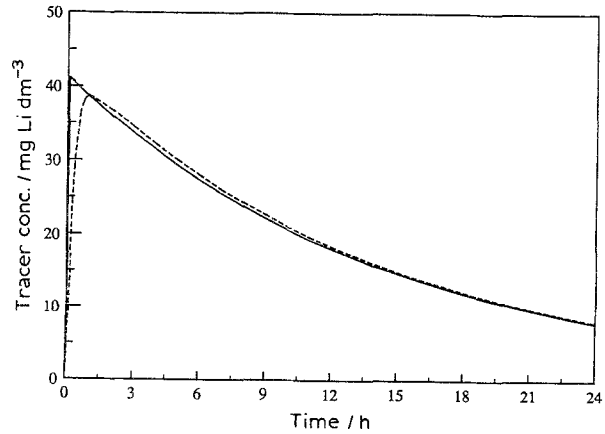

Fig. 3. Comparison of one and two-tank simulations of tracer test. Key: (– – – –) two-tank model; (———) one tank model.

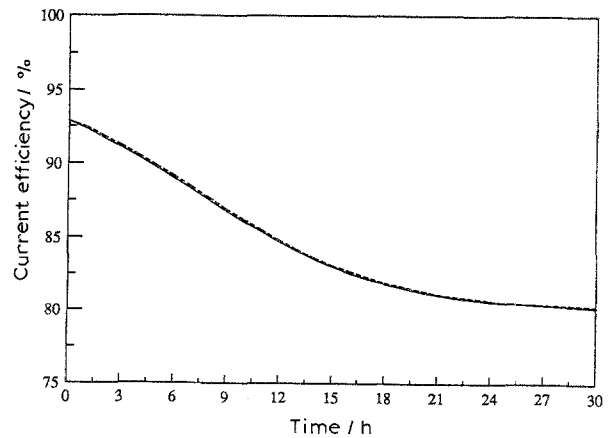

Fig. 5. Dynamic response of full-size cell to a step decrease in feed flowrate. Key: (– – – –) two-tank model; (———) one tank model.

time, this model can predict full-size cell performance as accurately as the available experimental equipment and significantly more quickly. The model can also be used to look at the economic optimization of both existing and proposed electrowinning circuits, as well as the dynamic behaviour of cells both with and without controllers. These applications of the full-size cell model will be described in the last paper in this series.

4. Conclusions

A (dynamic) mathematical model has been developed for a full-size zinc electrowinning cell operating with a high purity feed, by scaling-up the model of a (10 dm^3) pilot-plant cell. All of the scale-up effects considered were relatively small in magnitude. Some (such as the effect of an increased number of bubbles on electrolyte conductivity and, hence, on cell voltage) did not warrant the increased model complexity that their inclusion would entail. Those effects included in the model only required readily obtainable data from a full-size cell. The important point here is that because the underlying pilot-plant model already contained the fundamental mass and energy balances together with the reaction kinetics and thermodynamics of the system, it could readily be scaled-up.

Both the pilot-plant and the full-size cell models share common limitations which should be realized. Firstly, they were developed for a particular zinc refinery and while the modelling approach and equations will not change between sites, some of the experimentally determined model parameters certainly will. Secondly, the models do not account for the effects of different additives or additive levels. Experimental work [6] has shown that these can have a significant effect on cell performance, but in these models it is merely assumed that an 'adequate' additive mixture is used. Finally, the models are primarily steady-state in nature. Only cell electrolyte (not cell electrode) dynamics are incorporated in the models, and even these dynamics have only been qualitatively validated. Despite its limitations, however, the full-size cell model satisfies its major original objective, *viz* to provide an accurate tool that can be usefully employed in analysis and design studies at both the cell and the electrowinning circuit levels.

Acknowledgements

The authors of this paper would like to thank the Electrolytic Zinc Company and the CSIRO, Division of Mineral and Process Engineering, for their financial and technical support of the work reported in this paper.

References

[1] A. C. Scott, R. M. Pitblado, G. W. Barton and A. R. Ault, *J. Appl. Electrochem.* **18** (1988) 120–7.
[2] G. W. Barton and A. C. Scott, *J. Appl. Electrochem.* **22** (1992) 104–15.
[3] C. C. Pantelides, *Comp. Chem. Eng.* **12** (1988) 745–55.
[4] A. Hills and J. Szekely, *Chem. Eng. Sci.* **19** (1964) 79–81.
[5] T. Kumada, F. Kasahara and R. Ishiguro, *J. Nucl. Sci. Technol.* **13** (1976) 74–80.
[6] A. C. Scott, 'The Development and Application of a Mathematical Model for the Zinc Electrowinning Process', Ph.D. Thesis, University of Sydney, Australia (1988).
[7] P. J. Sides, AIChE Symposium Series No. 229, **79** (1983) 226–32.
[8] G. Kreysa and M. Kuhn, *J. Appl. Electrochem.* **15** (1985) 517–26.
[9] J. R. Rawling and L. D. Costello, *J. Metals*, May (1969) 49–52.